AIP | Journal of Applied Physics

A study of magnetic ordering in multiferroic hexagonal Ho1- x Dy x MnO3

J. Magesh, P. Murugavel, J. Krishnamurthy, V. Adyam, and W. Prellier

Citation: Journal of Applied Physics **117**, 074104 (2015); doi: 10.1063/1.4913219
View online: http://dx.doi.org/10.1063/1.4913219
View Table of Contents: http://scitation.aip.org/content/aip/journal/jap/117/7?ver=pdfcov
Published by the AIP Publishing

JOURNAL OF APPLIED PHYSICS **117**, 074104 (2015)

A study of magnetic ordering in multiferroic hexagonal $Ho_{1-x}Dy_xMnO_3$

J. Magesh,[1] P. Murugavel,[1,a)] J. Krishnamurthy,[2] V. Adyam,[2] and W. Prellier[3]
[1]*Department of Physics, Indian Institute of Technology Madras, Chennai 600036, India*
[2]*Cryogenic Engineering Centre, Indian Institute of Technology Kharagpur, Kharagpur 721302, India*
[3]*Laboratoire CRISMAT, ENSICAEN, CNRS UMR 6508, 6 Bd Maréchal Juin, 14050 Caen, France*

(Received 4 December 2014; accepted 5 February 2015; published online 19 February 2015)

This paper investigates the magnetic properties of $Ho_{1-x}Dy_xMnO_3$ by considering the inter-planar Mn^{3+}-O-O-Mn^{3+} interaction. The theoretical analysis shows that the asymmetric in-plane exchange interaction couples the in-plane and inter-planar Mn^{3+} spin structures via asymmetry parameter δ. This leads to the existence of both the in-plane and inter-planar ordering, which in turn restricted the allowed magnetic space groups to Γ_1 and Γ_4. The experimental studies confirmed the concomitant nature of the in-plane and the inter-planar ordering at T_N, T_{SR}, and T_2. It also showed that the magnetic phase diagram is dominated by the allowed magnetic structures Γ_1 and Γ_4. Furthermore, an effort is made to resolve the inconsistency regarding the T_{SR} (32 or 40 K). The studies revealed that the antiferromagnetic inter-planar interaction is switched to the ferromagnetic interaction (40 K) upon cooling, which in turn drives the spin reorientation at 32 K. The Mn^{3+} spin structure is seen to be coupled to rare earth sub-lattice through the modulation of the inter-planar interaction. © *2015 AIP Publishing LLC*. [http://dx.doi.org/10.1063/1.4913219]

I. INTRODUCTION

Among the multiferroic hexagonal $RMnO_3$,[1–3] $HoMnO_3$ has received lot of attention due to its rich magnetic phase diagram.[4–8] However, the magnetic phase diagram of $HoMnO_3$ is mostly inferred indirectly from dielectric and specific heat measurements due to the masking effect of high paramagnetic Ho^{3+} moment. The Mn^{3+} spins align in a frustrated triangular antiferromagnetic fashion in the *ab*-plane with spins either parallel (Γ_1 and Γ_3) or perpendicular (Γ_2 and Γ_4) or oriented (Γ_5 and Γ_6) at an angle to the in-plane axis. There are two such layers of spin alignments with the inter-layer coupling being either ferromagnetic (α-structures) or antiferromagnetic (β-structures) in nature. This results in six possible magnetic structures (Γ_1, Γ_2, Γ_3, Γ_4, Γ_5, and Γ_6).[9,10] However, Mn^{3+} is believed to undergo only two dimensional in-plane antiferromagnetic ordering. The inter-planar Mn^{3+} ordering is ignored by considering that it is weak by two orders of magnitude.[11] Note that the inter-planar Mn^{3+}-O-O-Mn^{3+} separation (6.5 Å) is almost twice the in-plane Mn^{3+}-O-Mn^{3+} (3.5 Å) distance.[12] But the inter-planar Mn^{3+}-O-O-Mn^{3+} interaction and the resultant ordering are the ones which differentiate the α (ferromagnetic for Γ_1 and Γ_2) and β (antiferromagnetic for Γ_3 and Γ_4) structures. Nevertheless, the high frustrating factor of $RMnO_3$ drastically reduces the T_N by a factor of 10, which brings out the role of inter-planar Mn^{3+}-O-O-Mn^{3+} magnetic interaction into consideration at these temperatures. Hence, in the present work the inter-planar ordering is considered while re-examining the magnetic phase diagram of $HoMnO_3$.

The $HoMnO_3$ undergoes three magnetic transitions at 70 K, 32 K, and 5 K, respectively. The transitions at 70 K and 5 K are attributed to antiferromagnetic ordering of Mn^{3+} (T_N) and Ho^{3+}(T_2), respectively.[13] Though the researchers agree on the 90° Mn^{3+} in-plane spin reorientation (T_{SR}) at 32 K,[4–6,9,10,14] they differ in attributing the magnetic space group and the driving force behind T_{SR}. There are reports on complete rare earth ordering driven spin reorientations and also partial rare earth ordering driven spin reorientations at T_{SR}.[4,5,14] In addition, a vast inconsistency is prevalent in the literature on the spin reorientation temperature itself. Lorentz *et al.*[7] reported a spin reorientation at 32 K for $HoMnO_3$, whereas based on the dielectric measurements Zhou *et al.*[15] observed it at 40 K. The neutron diffraction and small angle neutron scattering suggest that the spin reorientation is at 40 K.[6,16] However, the inconsistency was simply consigned to sample preparation technique, but a careful scrutiny of the literature let one conclude that the discrepancy is innate response of the sample and has nothing to do with sample preparation method. Though the researchers agree that the transition associated with 32 K is spin reorientation, the uncertainty remains regarding the transition around 40 K. The discrepancy can be reconciled by considering the spin reorientation is a gradual transition but the reported sharp peak in the dielectric constant of the single crystal at T_{SR} rules out the possibility of a gradual transition.[7,15] Signatures of such double transition are even observed at T_N and T_2. Hence, a comprehensive analysis of the magnetic phase diagram of $HoMnO_3$ is required.

II. THEORETICAL MODEL

The conventional tools like elastic neutron diffraction cannot differentiate the homometric pairs of magnetic structures (Γ_1 and Γ_3) and (Γ_2 and Γ_4).[16] However, Fabreges *et al.*[17] were able to reveal the change of inter planar structure based on the inelastic neutron scattering. In their theory, they conclude that the inter-plane interaction occurs independently irrespective of in-plane interaction, which suggests that they cannot explain the coupling between the in-plane and

a)Electronic mail: muruga@iitm.ac.in

inter-planar interaction. In the absence of such coupling, the theory allows all the four magnetic structures (Γ_1, Γ_2, Γ_3, and Γ_4), contrary to the experimental observation of the two magnetic structures (Γ_1 and Γ_4) in the phase diagram of RMnO$_3$. However, in P6$_3$cm structure, as the Mn^{3+} position deviates from the ideal $x_{Mn} = 1/3$, the asymmetric nature of the in-plane exchange interaction needs to be included. As a consequence, our work, where we consider the asymmetric in-plane exchange interaction, could elucidate the coupling between the in-plane and the inter-planar interaction.

The Hamiltonian of the two layers of triangular spin structure is $H = H_P + H_{IP}$. The in-plane Hamiltonian is $H_P = \Sigma_{i,j=1,2,3} J \mathbf{S}_i \cdot \mathbf{S}_j + \Sigma_{i,j=4,5,6} J \mathbf{S}_i \cdot \mathbf{S}_j$ and inter-planar Hamiltonian is $H_{IP} = \Sigma_{i=1,2,3;j=4,5,6} J_z \mathbf{S}_i \cdot \mathbf{S}_j$, where J and J_z are in-plane and inter-planar nearest neighbour exchange interaction energy, respectively. By assuming symmetric in-plane interaction, Fabreges *et al.*[17] obtained the interaction energy $\xi = 3/2S^2 + (J_{z1}–J_{z2})\mathbf{S}_3 \cdot \mathbf{S}_4$ and suggested that the inter-planar interaction can occur independently irrespective of the in-plane interaction. However, in hexagonal P6$_3$cm structure, as x_{Mn} deviates from 1/3 by $\pm\delta$, it becomes isosceles triangular lattice as shown in Fig. 1. Such asymmetric in-plane exchange interaction is also revealed in the Raman studies on hexagonal RMnO$_3$ thin film.[18] Considering the asymmetric in-plane interaction, the interaction energy is $\xi = (J_1–J_2)\mathbf{S}_2 \cdot \mathbf{S}_3 + (J_{z1}–J_{z2})\mathbf{S}_3 \cdot \mathbf{S}_4$ with the constraint $(d_{24})^2–(d_{34})^2 = \pm(3\sqrt{2})a\delta$, where d_{24} and d_{34} are the inter-planar Mn^{3+} distances and a is the side of the ideal triangular lattice (shown by dotted dashed line in Figs. 1(b) and 1(c)). This constraint shows that as the in-plane distance increases (J_1 decreases), the inter-planar distance decreases (J_{z1} increases), which results in the coupling between the in-plane and the inter-planar spin structures. Thus, the concomitant nature of the in-plane spin reorientation and the change of inter-planar ordering is a consequence of asymmetric in-plane exchange interaction.

In addition, the prevalence of Γ_1 and Γ_4 in the magnetic phase diagram of RMnO$_3$ can also be understood based on the asymmetric in-plane exchange interaction. For a small δ, the change of in-plane interaction changes the inter-planar interaction instantly ($(d_{24})^2 – (d_{34})^2$ changes sign readily). This leads to the observation of Γ_2 or Γ_3 in a small region of the phase diagram. On the other hand, if δ is large, the change of in-plane interaction does not readily change the inter-planar interaction ($(d_{24})^2 – (d_{34})^2$ does not change sign readily). This leads to the observation of Γ_2 and Γ_3 through wider region of phase diagram. The asymmetry parameter δ is determined by the asymmetry of the C_3 site. In RMnO$_3$ (Y, Ho, and Lu), the C_3 site deviates from ideal C_{3V} by $<5°$ resulting in small δ. As a consequence, the Γ_1 and Γ_4 phases dominate the magnetic phase diagram of RMnO$_3$. For HoMnO$_3$ at T_N, $\delta < 0$, i.e., $x_{Mn} < 1/3$, then $J_1 > J_2$, consequently (J_{z1}–J_{z2}) is negative which leads to the antiferromagnetic inter-layer coupling (Γ_4) as shown in Fig. 1(c). Upon cooling, at 40 K, due to anomalous expansion of c-axis,[19] $\delta > 0$, i.e., $x_{Mn} > 1/3$, then $J_1 > J_2$, consequently (J_{z1}–J_{z2}) is positive which leads to the ferromagnetic interlayer coupling (Γ_1) as shown in Figure 1(b). The coupling between the in-plane and the inter-planar interaction reduces the allowed magnetic structures only to experimentally observed Γ_4 or Γ_1 in RMnO$_3$, and the magnetic structure changes from Γ_4 to Γ_1 at T_{SR}. Similarly, for YMnO$_3$ at T_N, $\delta > 0$ will have an inter-layer ferromagnetic alignment (Γ_1) at T_N which is in line with the magnetic structure of YMnO$_3$ reported by Fabreges *et al.*[17]

The existence of such in-plane and inter-planar ordering is observed in LuMnO$_3$, where the non-magnetic nature of Lu^{3+} allows these transitions discernible in magnetic measurements.[20] However, the observations of such in-plane and inter-planar orderings in HoMnO$_3$ are tricky, as the high paramagnetic moment of Ho^{3+} masks even the T_N let alone the inter-planar ordering. On the other hand, due to weak magneto electric coupling in HoMnO$_3$, the dielectric measurements do not reveal the complete magnetic phase diagram, since some of the magnetic transitions are not apparent. In order to enhance the strain mediated magnetoelectric coupling, we doped the HoMnO$_3$ with higher ionic radii Dy^{3+}, since it is expected to enhance the coupling by 30 times.[21] Thus, our dielectric studies on Ho$_{1-x}$Dy$_x$MnO$_3$ along with a method to eliminate the paramagnetic background enabled us to establish the concomitant nature of the in-plane and the inter-planar ordering and thereby revealed the complete coherent magnetic ordering in Ho$_{1-x}$Dy$_x$MnO$_3$.

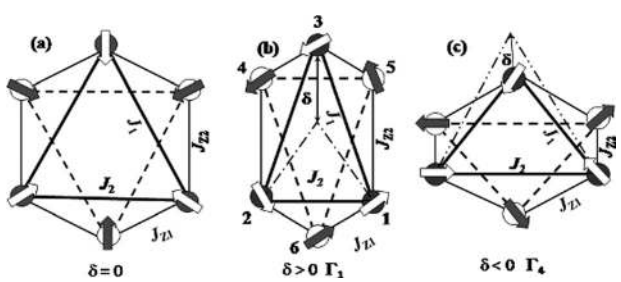

FIG. 1. Schematic representation of in-plane and inter-planar interaction between Mn^{3+} ions for the asymmetry parameter (a) $\delta = 0$, (b) $\delta > 0$, and (c) $\delta < 0$. Dark and dashed line represents triangular in-plane Mn^{3+} interactions at z = 0 and at z = ½, respectively. Solid line indicates the inter-planar interactions. Dotted dashed line represents the ideal triangular lattice of $\delta > 0$ and $\delta < 0$.

III. RESULTS AND DISCUSSION

A. In-plane (T_N) and inter-planar antiferromagnetic ordering ($T_{IP\text{-}AF1}$)

A series of Ho$_{1-x}$Dy$_x$MnO$_3$ ($x = 0$ to 1) samples were prepared by solid state routes. Powder x-ray diffraction (XRD) patterns obtained using PANANALYTIC X-ray diffractometer confirm the hexagonal structure for $x \leq 0.5$. The magnetization measurements were performed from 4 K to 300 K by applying 100 Oe under zero field cooled (ZFC) and field cooled (FC) conditions using Vibrating Sample Magnetometer in the Physical Property Measurement System. These measurements did not reveal any magnetic transitions due to high paramagnetic Ho^{3+} moments, in agreement with the earlier reports. However, the paramagnetic background is eliminated by obtaining the difference between ZFC and FC so as to reveal the Mn^{3+} ordering in the system.

Figure 2(a) shows the ZFC-FC data as a function of temperature for $x = 0.1$, 0.3, and 0.5. The graphs show three humps, for example, at 73 K, 67 K, and 63 K for $x = 0.1$ sample. The antiferromagnetic ordering will manifest as a hump in ZFC-FC, whereas the ferromagnetic ordering will be revealed as a hump in FC-ZFC. Hence, the humps at 73 K and 67 K are attributed to the in-plane antiferromagnetic transition T_N and inter-planar antiferromagnetic ordering $T_{IP\text{-}AF1}$, respectively. The origin of the third transition at 63 K is not yet clear. However, there is a clear indication of such transition in dielectric studies performed on our polycrystalline samples, and single crystalline samples[22] indicating it as a genuine magnetic phase transition.

Figure 2(b) shows the FC–ZFC data from 20 K to 50 K for $x = 0$, 0.1, 0.3, and 0.5. The hump in FC-ZFC around 35 K indicates the ferromagnetic ordering transition. In $P6_3cm$ crystal structure, ferromagnetic ordering of Mn^{3+} is allowed only along the inter-planar direction, whereas the in-plane interaction will always remain antiferromagnetic. The hump at 35 K is an evidence for the change of inter-planar Mn^{3+} interaction from antiferromagnetic ($T_{IP\text{-}AF1}$) to ferromagnetic($T_{IP\text{-}FM}$). However, the reported antiferromagnetic in-plane Mn^{3+} spin reorientation T_{SR1} is buried under the inter-planar ferromagnetic ordering. Note that the ZFC-FC at the antiferromagnetic ordering (T_N) is weaker by more than an order of magnitude compared to ferromagnetic ordering ($T_{IP\text{-}FM}$).

Upon Dy^{3+} substitution, the $T_{IP\text{-}FM}$ remains similar up to $x = 0.3$, above which it decreases. Such variation of $T_{IP\text{-}FM}$ with composition can explain the role of inter-planar coupling and rare earth ion in the spin reorientation. Rare earth occupies two different sites C_{3V} and C_3. The C_{3V} site which lies at the edge of the unit cell does not play a role in the inter-planar interaction. On the other hand, the C_3 site which lies well inside the unit cell modulates the inter-planar interaction. Our earlier studies on magnetoelectric coupling strength of Dy^{3+} substituted $HoMnO_3$ suggested a C_{3V} site specific substitution.[23] The Dy^{3+} preferentially occupies the C_{3V} site up to $x = 1/3$ and hence will not affect the inter-planar interaction. This results in a constant $T_{IP\text{-}FM}$ for $x \leq 0$. 3. Above $x = 1/3$, the higher ionic radii Dy^{3+} also replace the C_3 site, which resulted in the decrease of $T_{IP\text{-}FM}$ as observed for $x = 0.5$ in ZFC-FC data. The compositional variation of $T_{IP\text{-}FM}$ points out that the Dy^{3+} undergoes site specific substitution and the rare earth plays a role in the spin reorientation by modulating the Mn^{3+}-O-O-Mn^{3+} inter-planar interaction.

B. Interplanar ferromagnetic ordering ($T_{IP\text{-}FM}$) and the spin reorientation (T_{SR1})

To investigate it further, we measured the dielectric constant using Agilent 4248 RLC bridge coupled to PPMS. Figure 3(a) shows the temperature variation of dielectric constant and the loss factor at 50 kHz for $Ho_{0.9}Dy_{0.1}MnO_3$ sample. The dielectric constant shows a slope change at 27 K, 36 K, and 46 K. We suggest that in $Ho_{0.9}Dy_{0.1}MnO_3$, the Mn^{3+} in-plane spin reorientation T_{SR1} occurs at 27 K and the inter-planar ferromagnetic $T_{IP\text{-}FM}$ occurs at 36 K. The transition at 46 K is suggested as the consequence of the onset of lattice frustration, which drives the spin reorientation.

The two transitions which hitherto manifest in different set of measurements in $HoMnO_3$ are convincingly observed in $Ho_{0.9}Dy_{0.1}MnO_3$. Such revelation is mainly due to the strong enhancement of magnetoelectric coupling in the $Ho_{0.9}Dy_{0.1}MnO_3$ than that of $HoMnO_3$.[21] Additionally, the dielectric loss factor also reveals a broad peak around T_{SR1} and a sharp peak around $T_{IP\text{-}FM}$. In fact, there are abundance of studies in $HoMnO_3$ to suggest that the spin reorientation is a two step transition. For example, the T_{SR1} which is a single sharp transition broadens into a plateau region in an applied magnetic field.[7] The neutron diffraction studies reveal the signature of double transition even in the absence of the external field.[6] The polarization shows a sharp decrease at $T_{IP\text{-}FM}$ (40 K) followed by a slope change at T_{SR1}(32 K).[24] The muon spin relaxation shows double transitions with two different relaxation rates corresponding to in-plane (*ab*-plane) and inter-planar ordering (*c*-axis), respectively.[25] The magnetic measurements on thin films also imply that the T_{SR} is accompanied by another transition.[26] Our studies reconcile the discrepancy in T_{SR} by revealing it as a two-step transition

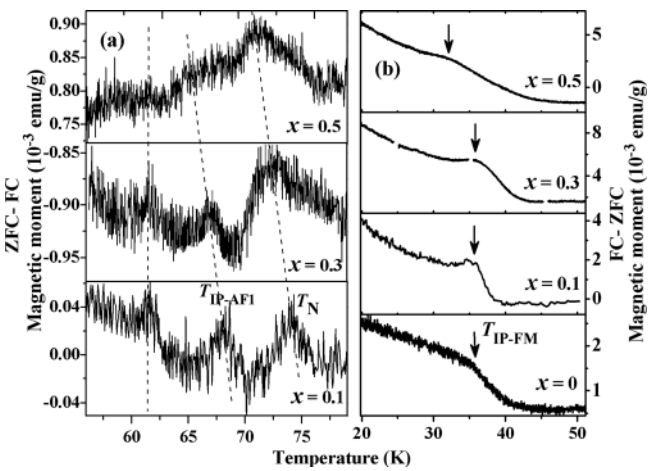

FIG. 2. The ZFC-FC data near (a) T_N and (b) T_{SR} for various compositions. (Note that the y-axis is FC-ZFC in Figure 2(b)). The $T_{IP\text{-}FM}$ is marked by an arrow.

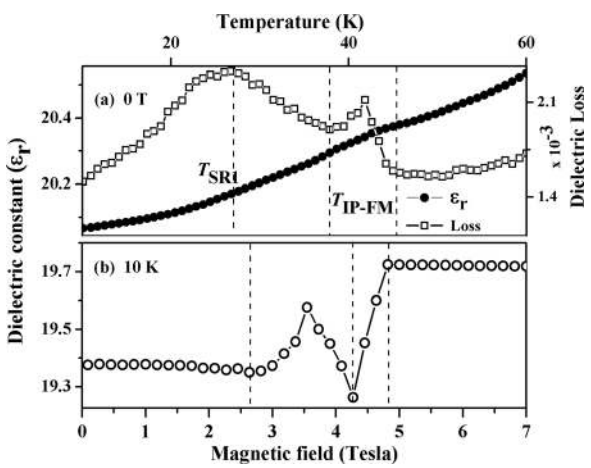

FIG. 3. (a) Dielectric constant and dielectric loss of $Ho_{0.9}Dy_{0.1}MnO_3$ as a function of temperature. (b) Dielectric constant versus field for $Ho_{0.9}Dy_{0.1}MnO_3$.

comprising the change of inter-layer coupling ($\Gamma_4 \rightarrow \Gamma_2$), which in turn drives the spin reorientation ($\Gamma_2 \rightarrow \Gamma_1$). The concomitant nature of inter-layer ordering and spin reorientation observed around 40 K and 5 K is expected to reflect in the reported high magnetic field spin reorientation as well.

To confirm this hypothesis, we measured the dielectric constant as a function of magnetic field for $Ho_{0.9}Dy_{0.1}MnO_3$ at 10 K, and the result is shown in Fig. 3(b). The phase diagram of $HoMnO_3$ suggests the change of magnetic phases at 2.5 T and 3.5 T upon sweeping the magnetic field.[7] Though these transitions are not clearly seen in polycrystalline $HoMnO_3$ sample, the doped $Ho_{0.9}Dy_{0.1}MnO_3$, due to strong magnetoelectric coupling, shows sharp change in dielectric constant around these transitions. Fig. 3(b) reveals that the dielectric constant remains same up to 2.7 T indicating the Γ_1 structure, and its peaks at 3.5 T suggesting the onset of spin reorientation at 2.7 T and the spin reorientation completes at 4.2 T (Γ_2). The dip in the dielectric constant at 4.2 T can be correlated to the change in *c*-axis after the spin reorientation which may favor a change in inter-planar interaction. Such change of inter-layer coupling results in dielectric constant jump around 4.8 T and remains constant thereafter (Γ_4). The jump in the dielectric constant upon the magnetic phase change ($\Gamma_2 \rightarrow \Gamma_4$) is in line with the sudden increase in polarization near 40 K ($\Gamma_2 \rightarrow \Gamma_4$).[24]

C. Spin reorientation (T_{SR2}) and inter-planar antiferromagnetic ordering ($T_{IP\text{-}AF2}$)

Figure 4(a) shows the magnetization versus temperature graphs for $HoMnO_3$ sample measured below 6 K under ZFC and FC conditions. Even though the transition at 5 K is attributed to the rare earth ordering,[27] as the transition is a re-entrant phase above 40 K, it is quite possible that it can originate from the in-plane spin reorientation followed by the inter-planar ordering. Thus, a careful scrutiny of this transition has been done along with the reported single crystal data. Figure 4(c) shows the inverse susceptibility of $Ho_{1-x}Dy_xMnO_3$ from 2 K to 6 K. The plot indicates the presence of three magnetic orderings near 5 K with a temperature interval of 0.3 K. Similar three transitions are reported in single crystal[28] with the one along the *a*-axis and the others along the *c*-axis indicating their origin from the in-plane and inter-planar ordering, respectively. The increase in magnetic moment at 5.3 K shown in Fig. 4(b) precludes the Ho^{3+} antiferromagnetic ordering along the *c*-axis as it is expected to show a sharp fall in magnetic moment due to the suppression of its high paramagnetic moment. As the transition at 5 K is observed in the *ab*-plane, it could be attributed to the in-plane reorientation of the Mn^{3+} by another 90°.

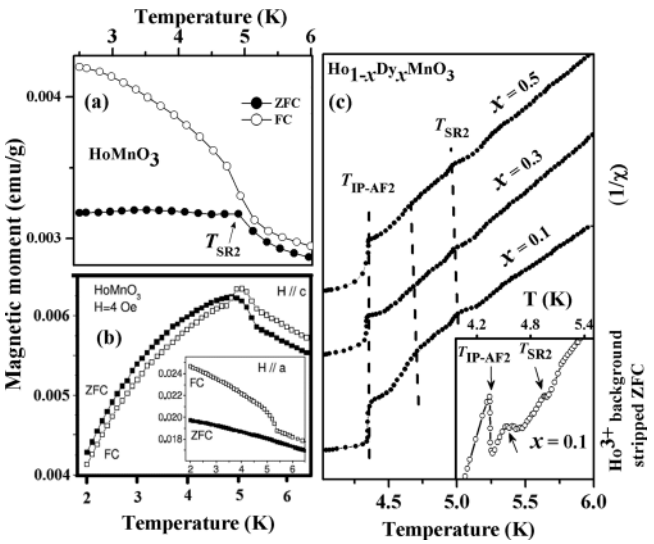

FIG. 4. (a) Magnetic moment *vs.* temperature of $HoMnO_3$. (b) The ZFC and FC of single crystal $HoMnO_3$. Reprinted with permission from E. Galstyan *et al.*, J. Phys.: Condens. Matter **20**, 325241 (2008) Copyright 2008 IOP Publishing. (c) The $1/\chi$ *vs.* temperature plots for $Ho_{1-x}Dy_xMnO_3$ samples (the inset shows ZFC data for $x = 0.1$ after paramagnetic Ho^{3+} background subtraction).

The transition at 4.7 K, observed only along the *c*-axis in single crystal, shows a sign change in FC-ZFC. This indicates that the ferromagnetic component changes into antiferromagnetic. Similar to the transition at $T_{IP\text{-}FM}$ (near T_{SR1}), the onset of sign change in FC-ZFC data (Fig. 4(b)) gives a strong evidence for change of inter-planar interaction from ferromagnetic to antiferromagnetic at T_{SR2}. The resultant re-entrant phase behaviour confirms the concomitant nature of the inter-planar ordering T_{IP} and the spin reorientation T_{SR}. The T_{SR2} and $T_{IP\text{-}AF2}$ transitions are clearly seen in $1/\chi$ plots shown in Fig. 4(c) for doped samples. The third transition at 5 K is probably due to rare earth ordering. These transitions are even more prominent in paramagnetic Ho^{3+} background striped χ plot shown in the inset of Fig. 4(c) for $Ho_{0.9}Dy_{0.1}MnO_3$.

Ample evidences are present in the literature to support that the inter-planar separation indeed decides the magnetic phases of the rare earth manganites. In $HoMnO_3$, the decrease of T_{SR} with applied pressure can be correlated to the suppression of elongation along the *c*-axis ($\delta < 0$). The *c*-axis suppression favors the antiferromagnetic inter-planar interaction thereby reducing the $T_{IP\text{-}FM}$ and consequently the T_{SR}.[19] In case of $YMnO_3$, as the inter-layer separation is already large ($\delta > 0$), it does not exhibit the spin reorientation even in the presence of a magnetic field. However, the inter-layer separation can be decreased by applying the pressure, i.e., $\delta < 0$. Such pressure induced spin reorientation is reported for $YMnO_3$.[29]

IV. CONCLUSIONS

In summary, the experimental and theoretical studies revealed the presence of inter-planar ordering near all the in-plane ordering temperatures T_N, T_{SR}, and T_2 confirming the concomitant nature of in-plane and inter-planar ordering. The results suggest that the lattice couples the spin structures via the in-plane and inter-planar ordering. As a result, the Γ_4 and Γ_1 magnetic phases dominate the phase diagram. Our studies give a coherent picture for the existence of various magnetic ordering in $HoMnO_3$ by considering the inter-planar interaction. Thus, the spin structure, the inter-planar ordering, and the magneto electric coupling strength are strongly coupled to the R^{3+} sub-lattice through the modulation of inter-layer Mn^{3+}-O-O-Mn^{3+}interaction.

ACKNOWLEDGMENTS

We thank the MSRC, IIT Madras where the magnetic measurements have been carried out. Partial support from the LAFCIS program and the CNRS is also acknowledged.

[1]Z. J. Huang, Y. Cao, Y. Y. Sun, Y. Y. Xue, and C. W. Chu, Phys. Rev. B **56**, 2623 (1997).
[2]D. G. Tomuta, S. Ramakrishnan, G. J. Nieuwenhuys, and J. A. Mydosh, J. Phys.: Condens. Matter **13**, 4543 (2001).
[3]T. Katsufuji, S. Mori, M. Masaki, Y. Moritomo, N. Yamamoto, and H. Takagi, Phys. Rev. B **64**, 104419 (2001).
[4]A. Munoz, J. A. Alonso, M. J. Martinez-Lope, M. T. Casais, J. L. Martinez, and M. T. Fernandez-Diaz, Chem. Mater. **13**, 1497 (2001).
[5]M. Fiebig, C. Degenhardt, and R. Pisarev, J. Appl. Phys. **91**, 8867 (2002).
[6]O. P. Vajk, M. Kenzelmann, J. W. Lynn, S. B. Kim, and S.-W. Cheong, Phys. Rev. Lett. **94**, 087601 (2005).
[7]B. Lorenz, A. P. Litvinchuk, M. M. Gospodinov, and C. W. Chu, Phys. Rev. Lett. **92**, 087204 (2004).
[8]B. Lorenz, F. Yen, M. M. Gospodinov, and C. W. Chu, Phys. Rev. B **71**, 014438 (2005).
[9]E. F. Bertaut and M. Mercier, Phys. Lett. **5**, 27 (1963).
[10]P. J. Brown and T. Chatterji, J. Phys.: Condens. Matter **18**, 10085 (2006).
[11]Th. Lonkai, D. G. Tomuta, J.-U. Hoffmann, R. Schneider, D. Hohlwein, and J. Ihringer, J. Appl. Phys. **93**, 8191 (2003).
[12]D. P. Kozlenko, S. E. Kichanov, S. Lee, J.-G. Park, V. P. Glazkov, and B. N. Savenko, Crystallogr. Rep. **52**, 407 (2007).
[13]H. Sugie, N. Iwata, and K. Khon, J. Phys. Soc. Jpn. **71**, 1558 (2002).
[14]Th. Lonkai, D. Hohlwein, J. Ihringer, and W. Prandl, Appl. Phys. A: Mater. Sci. Process **74**, s843 (2002).
[15]H. D. Zhou, J. Lu, R. Vasic, B. W. Vogt, J. A. Janik, J. S. Brooks, and C. R. Wiebe, Phys. Rev. B **75**, 132406 (2007).
[16]B. G. Ueland, J. W. Lynn, M. Laver, Y. J. Choi, and S.-W. Cheong, Phys. Rev. Lett. **104**, 147204 (2010).
[17]X. Fabreges, S. Petit, I. Mirebeau, S. Pailhès, L. Pinsard, A. Forget, M. T. Fernandez-Diaz, and F. Porcher, Phys. Rev. Lett. **103**, 067204 (2009).
[18]X.-B. Chen, N. T. Minh Hien, D. Lee, S.-Y. Jang, T. W. Noh, and I.-S. Yang, Appl. Phys. Lett. **99**, 052506 (2011).
[19]C. dela Cruz, F. Yen, B. Lorenz, Y. Q. Wang, Y. Y. Sun, M. M. Gospodinov, and C. W. Chu, Phys. Rev. B **71**, 060407 (2005).
[20]H. J. Lewtas, A. T. Boothroyd, M. Rotter, D. Prabhakaran, H. Müller, M. D. Le, B. Roessli, J. Gavilano, and P. Bourges, Phys. Rev. B **82**, 184420 (2010).
[21]J. Magesh, P. Murugavel, R. V. K. Mangalam, K. Singh, Ch. Simon, and W. Prellier, Appl. Phys. Lett. **101**, 022902 (2012).
[22]T. A. Tyson, T. Wu, K. H. Ahn, S.-B. Kim, and S.-W. Cheong, Phys. Rev. B **81**, 054101 (2010).
[23]J. Magesh, P. Murugavel, R. V. K. Mangalam, K. Singh, Ch. Simon, and W. Prellier, J. Appl. Phys. **112**, 104116 (2012).
[24]N. Hur, I. K. Jeong, M. F. Hundely, S.-B. Kim, and S.-W. Cheong, Phys. Rev. B **79**, 134120 (2009).
[25]H. J. Lewtas, T. Lancaster, P. J. Baker, S. J. Blundell, D. Prabhakaran, and F. L. Pratt, Phys. Rev. B **81**, 014402 (2010).
[26]P. Murugavel, J.-H. Lee, D. Lee, T. W. Noh, Y. Jo, M.-H. Jung, Y. S. Oh, and K. H. Kim, Appl. Phys. Lett. **90**, 142902 (2007).
[27]X. M. Wang, C. Fan, Z. Y. Zhao, W. Tao, X. G. Liu, W. P. Ke, X. Zhao, and X. F. Sun, Phys. Rev. B **82**, 094405 (2010).
[28]E. Galstyan, B. Lorenz, K. S. Martirosyan, F. Yen, Y. Y. Sun, M. M. Gospodinov, and C. W. Chu, J. Phys.: Condens. Matter **20**, 325241 (2008).
[29]D. P. Kozlenko, S. E. Kichanov, E. V. Lukin, S. Lee, J.-G. Park, and B. N. Savenko, High Pressure Res. **30**, 252 (2010).